Pijaudier-Cabot, G. and Huerta, A., Finite Element Analysis of Bifurcation in Nonlocal Strain Softening Solids, *Computer Methods in Applied Mechanics and Engineering*, Vol. 90, Issues 1, 3, pp. 905-919, 1991

Finite element analysis of bifurcation in nonlocal strain softening solids

Gilles Pijaudier Cabot
Laboratoire de Mécanique et Technologie, ENS Cachan/CNRS/Université Paris VI and GRECO Géomatériaux, 61 avenue du Président Wilson, 94235 Cachan Cedex, France

Antonio Huerta
Dpto. de Matematica Aplicada III, Universitat Politecnica de Catalunya, Jordi Girona Salgado 31, 08034 Barcelona, Spain

Progressive damage in brittle heterogeneous materials produces at the macroscopic level strain softening from which theoretical difficulties arise (e.g. ill-posedness and multiple bifurcation points). This characteristic behavior favours spurious strain localization in numerical analyses and calls for the implementation of localization limiters, for instance nonlocal damage constitutive relations. The issue of possible (stable or unstable) equilibrium paths, multiple localization zones, and of the detection of bifurcation points has, however, never been addressed in the context of nonlocal constitutive laws. We extend here the eigenmode analysis and perturbation method proposed by De Borst to the study of the bifurcation and post-bifurcation response of discrete nonlocal strain softening solids. Numerical applications on beams show that bifurcation and instability may occur in the post-peak regime. As opposed to the case of local constitutive relations, the number of possible solutions at a bifurcation point is restricted due to the constraint introduced by the localization limiter and these solutions are shown to be mesh independent.

1. Introduction

Progressive cracking in concrete, ceramics and fiber-reinforced composites is often treated as strain softening in continuum mechanics. However, such constitutive relations favour spurious strain localization with an arbitrary wave length, failure without energy dissipation, and more generally ill-posedness of boundary value problems. These issues have been extensively discussed over the past years (see e.g. [1] for a recent state of the art survey). A possible remedy to spurious strain localization is the implementation of so-called localization limiters, i.e. constraint conditions which remove the indetermination on the size (width) of the localization zone. Different sorts of limiters exist: some of them are purely numerical techniques such as the artificial rate dependence [2], or the spectral overlay method in which the minimum band-width of the localization zone (or shear band) can be fixed arbitrarily [3]. Since the 'missing length', namely the width of the localization zone (or shear band), is assumed to be a material property, to incorporate this parameter directly in the constitutive

relations appears to be a more elegant method. As a consequence, the material becomes micropolar [4] or nonlocal [5–7]. In these types of constitutive relations, there is an internal length called characteristic length which controls the minimum width of the localization zone [8]. Numerical applications demonstrated that failure without energy dissipation could not occur with nonlocal models and that the results were mesh independent [7, 9]. Nevertheless, it is interesting to point out that in most example problems, the region in which strain localization occurs is always known in advance because of the presence of triggering defects or stress concentration. Localization is forced to develop in a specific region of the structure.

If the purpose of a localization limiter is to prevent strain localization to develop in an arbitrarily small volume of the solid, it does not prevent bifurcation to occur although it should restrain the number of possible solutions at a bifurcation point. The issue of possible (stable or unstable) equilibrium paths, of multiple localization zones, and of the detection of the inherent bifurcation points is addressed here in the context of nonlocal constitutive relations. We apply the numerical technique developed by De Borst [10, 11] for usual (local) constitutive relations to the study of the bifurcation and of the post-bifurcation response of nonlocal strain softening solids by the finite element method. The material is assumed to follow the nonlocal damage constitutive equation [12] which is easily implemented in a standard finite element code. This model is briefly presented in Section 2. The computation of the tangent stiffness operator of the discrete structure is also detailed. The bifurcation and stability analyses are developed in Section 3. The issue of non-symmetric tangent stiffness matrices is discussed and the original eigenvalue analysis due to De Borst is extended to this case. Numerical implementations in a layered beam finite element code are presented in the last section. The results demonstrate the usefulness of bifurcation analysis and of stability checking in computational failure mechanics.

2. Nonlocal continuous damage

Brittle heterogeneous materials such as concrete undergo progressive microcracking due to increasing applied strain. The macroscopic effect of damage can be represented by a single internal state variable, denoted as D, within the realm of continuous damage mechanics. Among the various constitutive equations which were proposed to model the response of concrete [13], we choose the simplest model in which D is assumed to be a scalar variable. Thus, the stress–strain relation reduces to

$$\sigma_{ij} = C_{ijkl}(1 - D)\varepsilon_{kl} , \tag{1}$$

in which σ_{ij} and ε_{kl} are the stress and strain components (i, j, k, l $\in$ [1, 3]), and C_{ijkl} are the stiffness moduli of the undamaged (isotropic) material. The damage variable, D, ranges from 0 initially to 1 when the material cannot sustain any stress (failure). At this point we can remark that more realistic formulations exist [13] in which damage induced anisotropy and damage induced inelastic strains are taken into account. The technique presented here uses, without loss of generality, (1), due to its simplicity; nevertheless, its extension to more sophisticated models is straightforward.

The growth of damage is a function of the average damage energy release rate Y, and of the

damage loading surface defined as

$$F(Y) = Y - \mathcal{K} \,, \tag{2}$$

$$\text{if } F(Y) < 0 \text{ or if } F(Y) = 0 \text{ and } \dot{F}(Y) < 0 \quad \text{then } \dot{D} = 0 \,, \tag{3a}$$

$$\text{if } F(Y) = 0 \text{ and } \dot{F}(Y) = 0, \text{ then } D = f(Y) = 1 - (1 + b_1(Y - Y_0) + b_2(Y - Y_0)^2)^{-1} \,. \tag{3b}$$

In (2), $\mathcal{K}$ is the hardening-softening parameter. At each point of the solid $\mathcal{K} = \sup(Y, Y_0)$ for all the previous history of loading. Y_0 is the initial threshold of damage, b_1 and b_2 are material parameters. In the paper, the following numerical values identified from a tension test on concrete have been chosen: $Y_0 = 6 \cdot 10^{-5}$ MPa, $b_1 = 605.4\,\text{MPa}^{-1}$, $b_2 = 5.4 \cdot 10^4\,\text{MPa}^{-2}$ with $E = 32000$ MPa and $\nu = 0.2$. E and ν are the Young's modulus and Poisson ratio of concrete, respectively. The corresponding response of the material under uniaxial tension is shown in Fig. 1(a).

The key difference between the classical (local) and nonlocal damage model is that damage is a function of the average damage energy dissipation rate Y instead of the local energy dissipation rate y. Y is defined as

$$Y(\boldsymbol{x}) = \frac{1}{V_r(\boldsymbol{x})} \int_V \alpha(\boldsymbol{s} - \boldsymbol{x}) y(\boldsymbol{s})\, \mathrm{d}\boldsymbol{s} \,, \quad V_r(\boldsymbol{x}) = \int_V \alpha(\boldsymbol{s} - \boldsymbol{x})\, \mathrm{d}\boldsymbol{s} \,, \tag{4}$$

where $V_r(\boldsymbol{x})$ is the so-called representative volume at point $\boldsymbol{x}$, V is the volume of the structure and the local energy release y is by definition (see e.g. [13])

$$y(\boldsymbol{s}) = -\frac{\partial \frac{1}{2}\sigma_{ij}(\boldsymbol{s})\varepsilon_{ij}(\boldsymbol{s})}{\partial D} = \tfrac{1}{2} C_{ijkl}\varepsilon_{ij}(\boldsymbol{s})\varepsilon_{kl}(\boldsymbol{s}) \,. \tag{5}$$

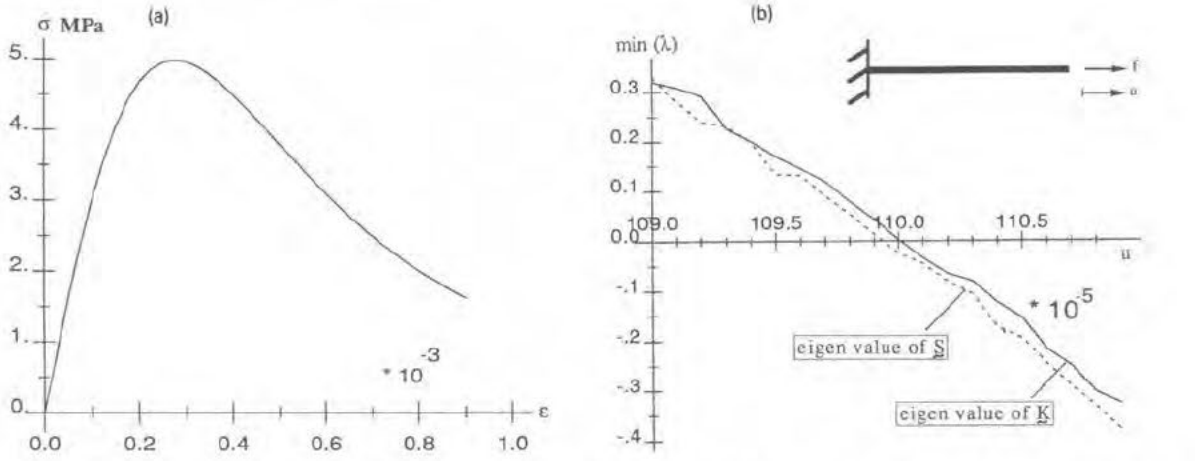

Fig. 1 (a) Stress–strain curve for concrete in tension. (b) Evolution of the minimum eigenvalue of $\boldsymbol{K}$ and $\boldsymbol{S}$ with the loading history for a clamped bar.

The physical justification for defining damage as a function of a nonlocal, i.e. average, quantity is fundamented by the existence of interactions among microcracks and between microcracks and heterogeneities (e.g. aggregate) in the material. The energy released when a microcrack propagates depends on these interactions and as a consequence the macroscopic effect of microcracking becomes nonlocal [14, 15]. From micromechanics, it is also possible to obtain the weighting function $\alpha(s-x)$ corresponding to simple crack configurations [14]. In this model, which was first proposed by Pijaudier-Cabot and Bazant [12], α is a weighting function that is chosen gaussian for numerical reasons: the rate of convergence of the finite element solution with respect to mesh refinement was observed to be maximum with a gaussian function compared to the rectangular or triangular weighting functions usually chosen [8].

$$\alpha(s-x)=\exp(-2\|s-x\|^2/l^2)\,, \tag{6}$$

$\|\ \|$ designates the euclidean norm and l is the characteristic length of the material which can be measured experimentally [16]. The weighting function is chopped in finite calculations: weights that are less than 0.001 are set to zero. Therefore, the actual volume of integration in (4) does not span over the entire volume of the solid. This assumption simplifies the computation of the average damage energy release rate in numerical applications: the number of neighboring points is greatly reduced and calculations are less time and memory consuming. Trial examples have shown that this assumption had very little effect on numerical results.

These constitutive relations have been implemented in a layered beam finite element code which uses a secant stiffness algorithm to solve the nonlinear system of equations (for details on the finite element model, see [17]). The nonlocal model is relatively easy to implement since the equilibrium equations are standard. The integral equation (4) is discretized according to the finite element mesh used for the analysis and a usual quadrature rule is employed for its evaluation. Since $\alpha(s-x)$ is independent of the boundary conditions, the numerical evaluation of (4) is further simplified: prior to initiate the calculations, the average weights are computed at each quadrature point and stored in a special file once and for all.

Although it has never been pointed out, there is a major reason for using a secant stiffness algorithm and not a usual tangent stiffness procedure for which the convergence properties can be checked. We can illustrate this by looking at the rate constitutive equations:

$$\dot{\sigma}_{ij}=C_{ijkl}(1-D)\dot{\varepsilon}_{kl}-C_{ijkl}\varepsilon_{kl}\dot{D}\,. \tag{7}$$

When the damage variable increases (i.e. when condition (3b) is satisfied), the rate of damage is

$$\dot{D}(x)=\frac{\partial f(Y)}{\partial Y}\cdot\frac{1}{V_r(x)}\int_V \alpha(s-x)C_{ijkl}\varepsilon_{ij}(s)\dot{\varepsilon}_{kl}(s)\,\mathrm{d}s\,. \tag{8}$$

We see that $\dot{D}(x)$ depends not only on the strain rate at point x but also on the strain rate at any point of the solid. Thus, a matrix of tangent material moduli cannot be calculated since the stress rate at point x depends on the strain rate everywhere in the solid. As a consequence, local conditions for strain localization such as the loss of ellipticity (singularity of the acoustic tensor) [18] or the complementing conditions [19] are difficult to derive. In the case of a

nonlocal solid, the rate equations of equilibrium are a system of nonlinear integral equations for which analytical solutions do not exist in the general case of a finite two-dimensional or three-dimensional solid. As it could be expected from the nature itself of the constitutive equations, the conditions for bifurcation and stability should derive from a global analysis of the boundary value problem, and cannot be approximated by local failure-detection criteria [18, 20].

Finally, we can also remark that the kernel in the integral equation (8) is non-symmetric. This property was first noticed in the study of strain localization in a one-dimensional bar whose material follows the nonlocal damage model [8]. Therefore, the tangent stiffness operator $\boldsymbol{K}$ which relates the nodal velocities to the rate of loading applied to the structure should also be non-symmetric.

Within the finite element method, the calculation of the tangent stiffness matrix $\boldsymbol{K}$ requires a special procedure. For simplicity, we will use in the following the customary contracted notation: $\sigma_{11} = \sigma_1, \ldots, \sigma_{23} = \sigma_4, \ldots, \varepsilon_{22} = \varepsilon_2, \ldots, 2\varepsilon_{13} = \varepsilon_5$, etc. Stresses and strains are denoted as the vectors $\boldsymbol{\sigma}$ and $\boldsymbol{\varepsilon}$, respectively, with six components each and the stiffness matrix is denoted as $\boldsymbol{C}$. Consider the incremental equations of equilibrium:

$$\int_V \boldsymbol{B}^{\mathrm{t}} \cdot \dot{\boldsymbol{\sigma}} \, \mathrm{d}\boldsymbol{x} = \dot{f} \quad \text{with } \dot{\boldsymbol{\varepsilon}} = \boldsymbol{B} \cdot \dot{\boldsymbol{u}} \,, \tag{9}$$

where $\boldsymbol{B}$ is the strain-nodal displacement matrix, $\dot{\boldsymbol{u}}$ is the vector of nodal velocities, superscript t denotes the transposition and $\dot{f}$ is the rate of loading (at each node). Substitution of the rate constitutive equations (7) into (9) yields

$$\int_V (1 - D)\boldsymbol{B}^{\mathrm{t}} \cdot (\boldsymbol{C} \cdot \boldsymbol{B}) \, \mathrm{d}\boldsymbol{x} \, \dot{\boldsymbol{u}} - \int_V \boldsymbol{B}^{\mathrm{t}} \cdot (\boldsymbol{C} \cdot \boldsymbol{\varepsilon}) \dot{D} \, \mathrm{d}\boldsymbol{x} = \dot{f} \,. \tag{10}$$

In this equation, the first integral on the left hand-side yields the secant stiffness matrix: we substitute now (8) into the second integral of (10):

$$\int_V \boldsymbol{B}^{\mathrm{t}} \cdot (\boldsymbol{C} \cdot \boldsymbol{\varepsilon}(\boldsymbol{x})) \dot{D}(\boldsymbol{x}) \, \mathrm{d}\boldsymbol{x} = \int_V \boldsymbol{B}^{\mathrm{t}} \cdot (\boldsymbol{C} \cdot \boldsymbol{\varepsilon}(\boldsymbol{x})) \left[\left\langle \frac{\partial f(Y)}{\partial Y} \right\rangle \int_V \frac{\alpha(\boldsymbol{s} - \boldsymbol{x})}{V_r(\boldsymbol{x})} \boldsymbol{\varepsilon}(\boldsymbol{s})^{\mathrm{t}} \cdot \boldsymbol{C} \cdot \dot{\boldsymbol{\varepsilon}}(\boldsymbol{s}) \, \mathrm{d}\boldsymbol{s} \right] \mathrm{d}\boldsymbol{x} \,. \tag{11}$$

$\langle \ \rangle$ in (11) stand for a condensed notation of the damage evolution conditions at points $\boldsymbol{x}$.

$$\langle A \rangle = A \quad \text{if } \dot{D}(\boldsymbol{x}) > 0 \,, \qquad \langle A \rangle = 0 \quad \text{if } \dot{D}(\boldsymbol{x}) = 0 \,.$$

The strain rates can now be expressed in function of the nodal velocities $\dot{\boldsymbol{u}}$:

$$\int_V \boldsymbol{B}^{\mathrm{t}} \cdot (\boldsymbol{C} \cdot \boldsymbol{\varepsilon}(\boldsymbol{x})) \dot{D}(\boldsymbol{x}) \, \mathrm{d}\boldsymbol{x}$$

$$= \int_V \boldsymbol{B}^{\mathrm{t}} \cdot (\boldsymbol{C} \cdot \boldsymbol{\varepsilon}(\boldsymbol{x})) \left[\left\langle \frac{\partial f(Y)}{\partial Y} \right\rangle \int_V \frac{\alpha(\boldsymbol{s} - \boldsymbol{x})}{V_r(\boldsymbol{x})} \boldsymbol{\varepsilon}(\boldsymbol{s})^{\mathrm{t}} \cdot (\boldsymbol{C} \cdot \boldsymbol{B}) \, \mathrm{d}\boldsymbol{s} \right] \mathrm{d}\boldsymbol{x} \cdot \dot{\boldsymbol{u}} \,. \tag{12}$$

The above integrals as well as the first integral in the left-hand side of (10) are computed

for each element and assembled into the matrix $\boldsymbol{K}$ such that $\boldsymbol{K}\dot{\boldsymbol{u}} = \dot{\boldsymbol{f}}$. After some algebra, the generic expression of the stiffness matrix $\boldsymbol{K}_k$ of element k in the local coordinates attached to this element is

$$\boldsymbol{K}_k = [-\boldsymbol{D}_{k1}, -\boldsymbol{D}_{k2}, \ldots \boldsymbol{C}_k, -\boldsymbol{D}_{kk}, \ldots, -\boldsymbol{D}_{kn}]^{\mathrm{t}} , \tag{13}$$

with

$$\boldsymbol{D}_{kj} = \int_{V_k} \boldsymbol{B}^{\mathrm{t}} \cdot (\boldsymbol{C} \cdot \boldsymbol{\varepsilon}(\boldsymbol{x})) \left[\left\langle \frac{\partial f(Y)}{\partial Y} \right\rangle \int_{V_j} \frac{\alpha(\boldsymbol{s} - \boldsymbol{x})}{V_r(\boldsymbol{x})} \, \boldsymbol{\varepsilon}^{\mathrm{t}}(\boldsymbol{s}) \cdot (\boldsymbol{C} \cdot \boldsymbol{B}) \, \mathrm{d}\boldsymbol{s} \right] \mathrm{d}\boldsymbol{x}$$

and (14)

$$\boldsymbol{C}_k = \int_{V_k} (1 - D) \boldsymbol{B}^{\mathrm{t}} \cdot \boldsymbol{C} \cdot \boldsymbol{B} \, \mathrm{d}\boldsymbol{x} ,$$

in which V_j and V_k are the volumes of element j and k, respectively, and n is the total number of finite elements in the mesh. For layered beam elements with 3 degrees of freedom per node (2 nodes per element), matrix $\boldsymbol{K}_k$ is a $6 \times 3(n+1)$ rectangular matrix and $\boldsymbol{D}_{kj}, \boldsymbol{C}_k$ are 6×6 matrices. $\boldsymbol{D}_{kj}$ is the matrix of the moduli of interaction from element j on element k.

In general $\boldsymbol{D}_{kj} \neq \boldsymbol{D}_{jk}$; the loss of symmetry of $\boldsymbol{K}$ can be due to different loading conditions in element k and in element j:

$$\langle \partial f(Y) / \partial Y \rangle_{\text{in } k} \neq \langle \partial f(Y) / \partial Y \rangle_{\text{in } j} . \tag{15}$$

In particular, this condition is satisfied when element j is located inside the damage localization zone and element k is located outside this zone. The non-symmetry of $\boldsymbol{K}$ is also due to the weight function (non-symmetry of the kernel in (4)).

$$\alpha(\boldsymbol{s} - \boldsymbol{x}) / V_r(\boldsymbol{x}) \neq \alpha(\boldsymbol{x} - \boldsymbol{s}) / V_r(\boldsymbol{s}) . \tag{16}$$

For instance, when $\boldsymbol{x}$ lies near the boundary of the solid and point $\boldsymbol{s}$ is located inside the solid, the representative volumes $V_r(\boldsymbol{x})$ and $V_r(\boldsymbol{s})$ are not equal since the points lying outside the volume of the body are ignored in the calculation of the average damage energy release rate, and of the representative volume. Therefore, even when uniform damage exists (constant D over the solid), the tangent stiffness matrix is always non-symmetric.

In the finite element code, the matrix $\boldsymbol{K}$ is never used because it is non-symmetric and its bandwidth is much larger than the bandwidth of the secant stiffness operator. It is not a full matrix because weights that are less than 0.001 are set to zero and the corresponding terms in the interaction matrices become zero too. For the computation of equilibrium states, it appears easier to use a secant matrix, which is always symmetric. The matrix assembly remains standard too. Nevertheless, the tangent stiffness operator still needs to be calculated for analyzing stability and bifurcation of the discrete structure.

3. Bifurcation and stability of discrete systems

3.1. Loss of uniqueness

Uniqueness of the solution can be assessed by considering the incremental equations of equilibrium (9). For the sake of simplicity, attention is restricted to the case where the loading

is not stationary as bifurcation points and limit points rarely coincide (for a complete treatment of this problem see e.g. [10, 11]). If the solution of the rate boundary value problem is non-unique, the tangent stiffness matrix $\boldsymbol{K}$ should be singular:

$$\det \boldsymbol{K} = 0 . \tag{17}$$

However, $\boldsymbol{K}$ is not a single valued matrix. Depending on the strain rate field in the solid, damage may or may not grow in each element. Rigorously, all the possible (loading–unloading) combinations should be investigated. In the present applications, $\boldsymbol{K}$ is calculated for the incrementally linear comparison solid only. Our experience (for the examples presented in this paper) shows that the loss of uniqueness for the comparison solid occurs before it can be detected for any other loading–unloading configurations.

3.2. *Loss of stability*

At a state of equilibrium under dead load, a sufficient condition which guarantees stability of the structure is [21]

$$\int_V \dot{\boldsymbol{\sigma}}^{\mathrm{t}} \cdot \dot{\boldsymbol{\varepsilon}} \, \mathrm{d}\boldsymbol{x} > 0 \tag{18}$$

for all kinematically admissible strain rate field $\dot{\boldsymbol{\varepsilon}}$. Therefore, the equilibrium of a discrete system is critical if there exists a kinematically admissible field $\dot{\boldsymbol{u}}$ such that

$$\dot{\boldsymbol{u}}^{\mathrm{t}} \cdot \boldsymbol{K} \cdot \dot{\boldsymbol{u}} = 0 . \tag{19}$$

Again $\boldsymbol{K}$ is assumed to be single valued. This condition is equivalent to [10]

$$\det \boldsymbol{K} = 0 \quad \text{or} \quad \dot{\boldsymbol{u}} \text{ is orthogonal to } \boldsymbol{K}\dot{\boldsymbol{u}} . \tag{20}$$

The loss of stability does not necessarily occur at a bifurcation point because the tangent stiffness operator is not symmetric and in theory it may be possible to find a velocity field such that the second condition in (20) is satisified. Let us write the matrix $\boldsymbol{K}$ as the sum of a symmetric matrix $\boldsymbol{S}$ and an anti-symmetric matrix $\boldsymbol{T}$:

$$\boldsymbol{K} = \boldsymbol{S} + \boldsymbol{T} \quad \text{with } \boldsymbol{S} = \tfrac{1}{2}(\boldsymbol{K} + \boldsymbol{K}^{\mathrm{t}}) \text{ and } \boldsymbol{T} = \tfrac{1}{2}(\boldsymbol{K} - \boldsymbol{K}^{\mathrm{t}}) . \tag{21}$$

Equation (19) reduces to

$$\dot{\boldsymbol{u}}^{\mathrm{t}} \cdot \boldsymbol{K} \cdot \dot{\boldsymbol{u}} = \dot{\boldsymbol{u}}^{\mathrm{t}} \cdot \boldsymbol{S} \cdot \dot{\boldsymbol{u}} + \dot{\boldsymbol{u}}^{\mathrm{t}} \cdot \boldsymbol{T} \cdot \dot{\boldsymbol{u}} = \dot{\boldsymbol{u}}^{\mathrm{t}} \cdot \boldsymbol{S} \cdot \dot{\boldsymbol{u}} , \tag{22}$$

and the conditions (19) for the possible loss of stability become

$$\det \boldsymbol{S} = 0 . \tag{23}$$

Since the tangent matrix $\boldsymbol{K}$ is not symmetric, (23) must be met prior to (17). Matrix $\boldsymbol{K}$ could

also admit complex eigenvalues although it never happened in our calculations. However, it is not possible to demonstrate that for any solid, and any type of loading, complex eigenvalues cannot exist.

The determinants of matrix $\boldsymbol{K}$ and matrix $\boldsymbol{S}$ can be rewritten as the product of their eigenvalues λ_i and λ_i^s, respectively:

$$\det \boldsymbol{K} = \prod_{i=1}^{N} \lambda_i , \qquad \det \boldsymbol{S} = \prod_{i=1}^{N} \lambda_i^s , \tag{24}$$

where N is the total number of degrees of freedom of the system. Figure 1(b) shows the variation of the smallest eigenvalue as the loading progresses. The structure is a beam of length $L = 4l$ clamped at one end. The displacement along the neutral axis of the bar is imposed at the other extremity which is free to rotate and deflect. The variation of the minimum eigenvalues of $\boldsymbol{K}$ and $\boldsymbol{S}$, in which the rows and columns corresponding to fixed displacements have been removed, are plotted as functions of the imposed displacement. The figure shows the evolution of the eigenvalues for a small portion of the loading history near the peak load. We see that the condition for the loss of stability is met before the loss of uniqueness can occur. In fact, the real parts of the eigenvalues of $\boldsymbol{K}$ are bounded by the eigenvalues of $\boldsymbol{S}$ (see e.g. [20]):

$$\min(\lambda_i^s) \leqslant \min(\mathrm{Re}(\lambda_i)) . \tag{25}$$

The condition for the loss of stability is met at the peak load and bifurcation occurs later in the post-peak regime. The two conditions are very close to each other ($\boldsymbol{K}$ is 'weakly' non-symmetric), and only the criterion for loss of stability which is the lower bound will be used alone in the finite element code. It is also important to remark that the loss of stability (according to the criterion used) does not imply loss of uniqueness of the solution nor that the structure is necessarily unstable. The condition for stability in (18) is only necessary and it is only applied on the linear comparison solid. Conversely, at a bifurcation point, the structure will probably (although not necessarily) be unstable and we can see in Fig. 1(b) that the criterion which guarantees stability is not met at a bifurcation point.

3.3. *Post-peak and post-bifurcation response*

During the calculation and once the conditions for stability or uniqueness are not satisfied, it is necessary to investigate whether there exists a stable response of the structure and what the different possible paths in the post-bifurcation regime are. As the loading progresses, the loss of the stability condition is encountered first. For simplicity we assume that, at this point of the loading history, there is only one eigenvector denoted as $\boldsymbol{v}_1$ which is associated to the vanishing eigenvalue of S denoted as λ_1^s. Any velocity field $\dot{\boldsymbol{u}}$ which is collinear to $\boldsymbol{v}_1$ ($\dot{\boldsymbol{u}} = \gamma \boldsymbol{v}_1$) is such that

$$\gamma \boldsymbol{v}_1^{\mathrm{t}} \boldsymbol{K} \gamma \boldsymbol{v}_1 = 0 . \tag{26}$$

Since the loading rate $\dot{f}$ is fixed in the calculation, we know that there exists also a velocity

field denoted as $\dot{\boldsymbol{u}}^*$ which is the solution to the rate equilibrium problem:

$$\boldsymbol{K}\dot{\boldsymbol{u}}^* = \dot{\boldsymbol{f}} \,. \tag{27}$$

If the criterion for uniqueness is met, i.e. if $\boldsymbol{K}$ is non-singular which is the usual situation, then $\dot{\boldsymbol{u}}^*$ is unique. Consequently, the equilibrium of the structure is critical if $\dot{\boldsymbol{u}}^*$ is collinear to $\boldsymbol{v}_1$ and then the loading rate $\gamma \boldsymbol{K}\boldsymbol{v}_1$ should be statically admissible and should verify the essential boundary conditions (γ is a constant to be calculated). This property can be checked very easily: first we compute the loading vector $\boldsymbol{f}_1$ corresponding to $\boldsymbol{v}_1$:

$$\boldsymbol{K}\boldsymbol{v}_1 = \boldsymbol{f}_1 \,. \tag{28}$$

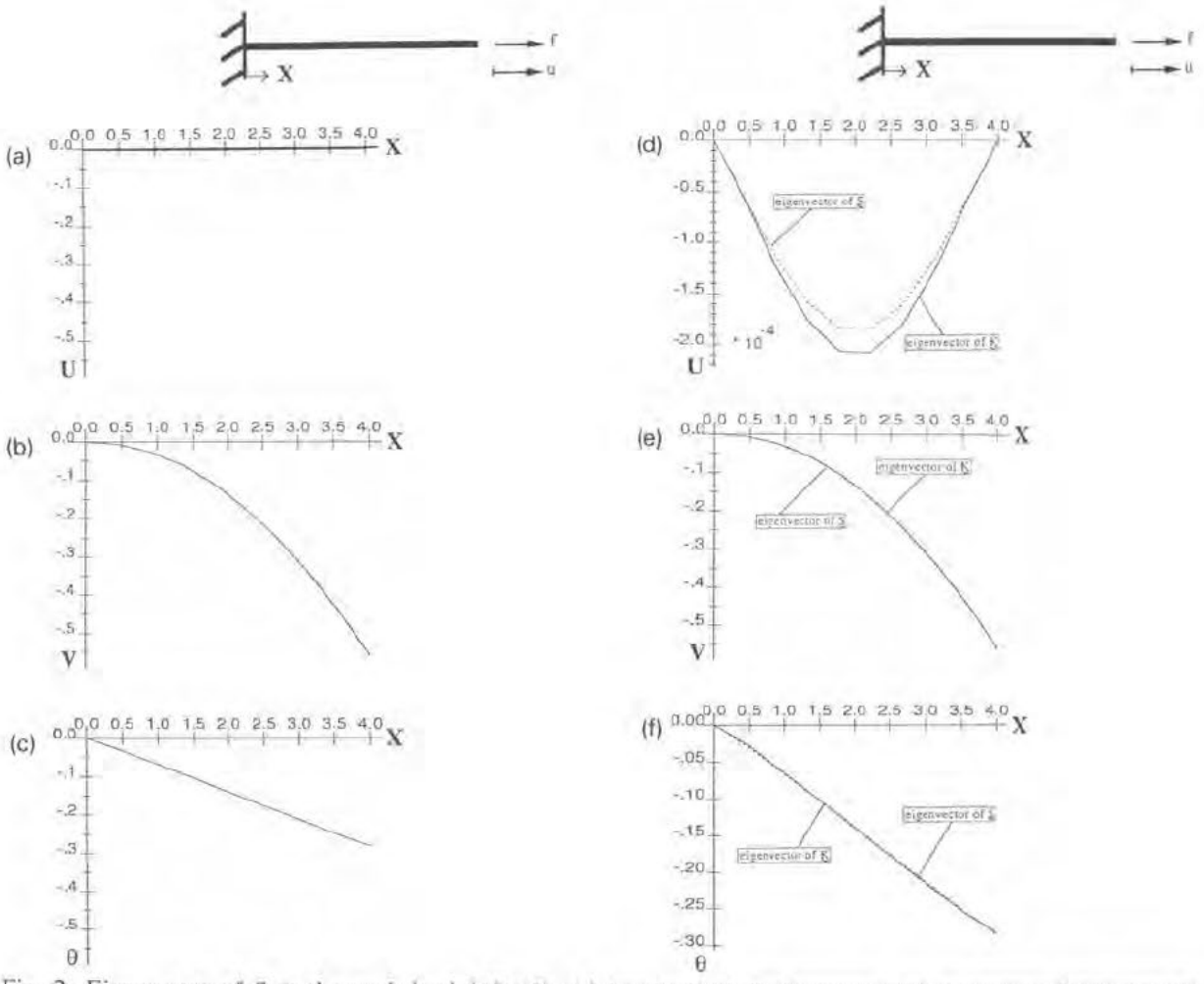

Fig. 2. Eigenvector of $\boldsymbol{S}$ at the peak load ($\lambda_1^s = 0$): (a) longitudinal displacement; (b) transverse displacement; (c) rotation; eigenvector of $\boldsymbol{S}$ and $\boldsymbol{K}$ at the bifurcation point ($\lambda_1^s = 0.0$–152, $\lambda_1 = 0$); (d) longitudinal displacement; (e) transverse displacement; (f) rotation.

Then f_1 is compared to $\dot{f}$ to see if there exists a scalar γ such that $\dot{f} = \gamma f_1$. In all the calculations that we have performed, $\dot{f}$ was never collinear to the loading rate. Fig. 2(a–c) shows the eigenvector calculated when $\lambda_1^S \cong 0$ for the clamped bar used in Section 3.2. Apart from the numerical errors, we see that the degrees of freedom which correspond to a displacement v parallel to the neutral axis of the beam are zero, while for instance the rotation θ increases linearly. For this structure, it is easy to check that a displacement field which is collinear to $\boldsymbol{v}_1$ cannot be a solution. Since the field of damage is uniform over the bar, for any non-zero scalar γ the load vector $\gamma \boldsymbol{K}\boldsymbol{v}_1$ should exhibit non-zero shear force and bending moment at the beam end. This is impossible according to the prescribed boundary conditions. In other words, when the distribution of damage is homogeneous over the beam, it cannot deflect if it is loaded in the direction of the neutral axis.

Let us now investigate the case where the criterion for uniqueness is not met: Again we know that there exists at least one solution $\dot{\boldsymbol{u}}^*$ to the rate equilibrium problem. Let us call this solution the fundamental solution. We denote as $\boldsymbol{\omega}_1$ the right eigenvector associated to the eigenvalue λ_1 of $\boldsymbol{K}$ which vanish. It can be demonstrated [10, 11] that for any arbitrary scalar β, the velocity field $\dot{\boldsymbol{u}}^* + \beta\boldsymbol{\omega}_1$ is also a solution of the problem

$$\boldsymbol{K}(\dot{\boldsymbol{u}}^* + \beta\boldsymbol{\omega}_1) = \dot{\boldsymbol{f}} . \tag{29}$$

Practically, it is extremely difficult to find at which point of the loading history either $\boldsymbol{S}$ or $\boldsymbol{K}$ becomes singular. During the numerical calculation, changes of sign of the eigenvalues are detected only, which means that between two increments of load, stability or uniqueness may be lost. Let $\boldsymbol{u}_{i-1}$ and $\boldsymbol{u}_i$ be the displacement field solutions of the equations of equilibrium at increments $i-1$ and i, and $\Delta\boldsymbol{u}_i$ the corresponding incremental displacement field between the two solutions. When an eigenvalue of $\boldsymbol{S}_i$, at increment i, has changed of sign and if stability is lost $\boldsymbol{u}_{i-1} + \gamma\boldsymbol{v}_1$ is an approximate solution at increment i. $\boldsymbol{u}_{i-1} + \Delta\boldsymbol{u}_i + \beta\boldsymbol{\omega}_1$ is an approximate solution too when uniqueness is lost and $\boldsymbol{K}$ is singular at a point in between increment $i-1$ and increment i. The fact that these solutions are only approximations should be stressed since the material behavior is nonlinear and $\boldsymbol{K}$ changes from one increment of load to the other. Nevertheless, these displacement fields are close enough to the real eigenvectors of $\boldsymbol{K}$ and $\boldsymbol{S}$ when these matrices are singular, and can serve as a new trial input denoted as $\boldsymbol{u}^t$ in the iterative process which yields to the solution at increment i [10]:

$$\boldsymbol{u}_1^t = \boldsymbol{u}_{i-1} + \gamma\boldsymbol{v}_1 + \beta\boldsymbol{\omega}_1 . \tag{30}$$

This type of perturbation would require the calculation of eigenvectors $\boldsymbol{v}_1$ and $\boldsymbol{\omega}_1$. $\boldsymbol{K}_i$ (at increment i) being non-symmetric, the calculation of $\boldsymbol{\omega}_1$ is lengthy and requires a lot of computer time and memory. The above perturbation method can be simplified.

Since the criterion for loss of stability is the most conservative, the eigenvalues of $\boldsymbol{S}_i$ (at increment i) are monitored only. When a negative eigenvalue is detected, the corresponding eigenvector is used in order to perturb the solution at increment i. This new trial solution is

$$\boldsymbol{u}^t = \boldsymbol{u}_i + \beta\boldsymbol{v}_1 . \tag{31}$$

Figure 2(d, f) shows a comparison of eigenvectors $\boldsymbol{v}_1$ and $\boldsymbol{\omega}_1$ for the example in Fig. 1(b). The

two eigenvectors are very similar. More importantly, the eigendisplacements $u(x)$ are non-zero which is consistent with the loss of uniformity of the field of damage in the beam. Therefore, the perturbation with $\boldsymbol{v}_1$ instead of $\boldsymbol{\omega}_1$ seems a reasonable approximation.

After this perturbation, a new solution is computed at increment i. Two possibilities exist:

- If a bifurcation point does not exist between increments i and $i-1$, the same solution $\boldsymbol{u}_i$ must be found and we must check that $\boldsymbol{v}_1$ is not collinear to $\Delta \boldsymbol{u}_i$, otherwise the structure is unstable and the analyst may wish to use another type of load control to overcome the loss of stability.
- If a new (different) solution is found for the equilibrium at increment i, an eigenvalue analysis is performed with the new value of matrix $\boldsymbol{S}_i$ in order to check that all eigenvalues are positive again (path stability).

When the symmetric operator $\boldsymbol{S}_i$ possesses several negative eigenvalues at the same load increment, the smallest eigenvalue is chosen for the perturbation and the above procedure is repeated until all the negative eigenvalues of $\boldsymbol{S}_i$ are either ignored (stability is not lost) or disappear.

The scalar β could be chosen arbitrarily. In order to accelerate the convergence toward the new solution, β is chosen so that the perturbed increment of the displacement field is orthogonal to the fundamental solution

$$\Delta \boldsymbol{u}^{\mathrm{t}} = \Delta \boldsymbol{u}_i + \beta \boldsymbol{v}_1 , \qquad \Delta \boldsymbol{u}^{\mathrm{t}} \perp \Delta \boldsymbol{u}_i \tag{32}$$

and

$$\beta = - \Delta \boldsymbol{u}_i^{\mathrm{t}} \cdot \Delta \boldsymbol{u}_i / \Delta \boldsymbol{u}_i^{\mathrm{t}} \cdot \boldsymbol{v}_1 . \tag{33}$$

4. Applications

Figure 3 shows the response of bars of different lengths subjected to tension. The length of the bar is proportional to the characteristic length of the material l ($L = 10l, 4l, 2l$). The finite elements have a constant length equal to $0.5l$. All the computations are displacement controlled and beyond the limit point the solution 'jumps' to complete failure. In this example, the deflections and rotations were prevented at each node. The average stress over the cross section of the bar is plotted as a function of the average strain over the entire bar u/L so that the curves can be compared to the stress–strain response of the material. As opposed to the case of local constitutive relations, the bifurcation point is always located beyond the peak load. The precise location of the bifurcation point depends on the bar length L. As L increases, the bifurcation point gets closer to the peak but only one eigenvalue becomes negative. There exist only two possible solutions: one in which the strain field is homogeneous, another one in which strains are non-uniform and tend to localize at the bar end. This is the result of the constraint effect introduced by the spatial averaging of the variable which controls the growth of damage. In the case of a local continuum, the number of negative eigenvalues would be proportional to the total number of elements in the finite element mesh. The stable path would further correspond to damage localization in a single finite element independently of its size [10].

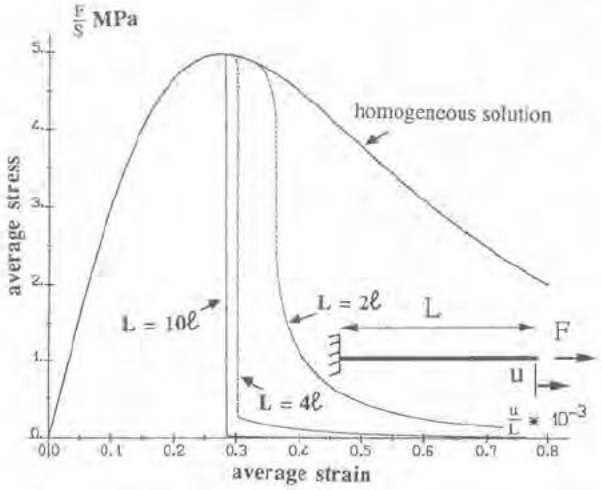

Fig. 3. Bar in tension: effect of the bar length on the post-bifurcation response.

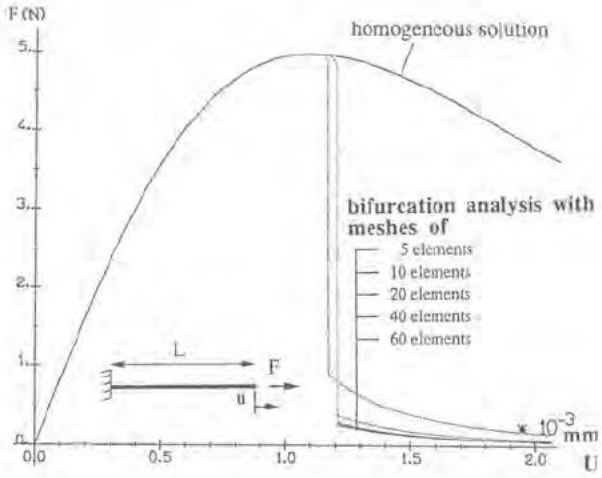

Fig. 4. Convergence of the finite element solution for a clamped bar with mesh refinement.

Figure 4 shows the responses calculated for a bar of length $4l$. Five different meshes with constant length elements have been used (5, 10, 20, 40 and 60 elements). We can observe a good convergence of the finite element solution with mesh refinement. For meshes with 10 elements and more, the response of the bar is approximately the same and the location of the bifurcation point becomes mesh independent. This result corroborates early convergence studies [8] in which it was observed that 3 elements are sufficient in the damage localization zone in order to get a close approximation of the analytical solution. The size of the damage localization zone is seen in Fig. 5, which presents for the same bar (20 elements) the evolution of the damage profiles at different load steps after the bifurcation point. When damage is no longer homogeneous over the whole bar, we can remark that it tends to localize progressively near one extremity of the bar until the limit point is reached. Then the structure becomes unstable and failure is reached in the elements near the right-hand side extremity of the bar where damage has reached its maximum value, 1.

In finite element analyses of bifurcation, it is also very important to check the influence of the shape functions used in the discretization as it may favour spurious eigenmodes or prevent bifurcation to occur. This influence is demonstrated in Fig. 6 for the same clamped bar of length $4l$. The previous calculation is compared to the computation in which each node is kept free to move perpendicularly to the neutral axis of the beam and to rotate. In the beam type solution, the damage field is not constrained to remain uniform over the element depth. Bifurcation occurs almost at the peak load and the distribution of damage at failure is not symmetric in each element with respect to their neutral axis. Damage localizes in the upper (or lower) corner of the extremity of the beam. Since the material stiffness is not uniform over the cross-section of the beam, the beam must deflect in order to accommodate the heterogeneity of the damage field. Note that this result is totally realistic; it was confirmed experimentally on tension specimens too [22]. This example underlines the importance of the finite element discretization, especially on the failure mode: if the kinematic corresponding to

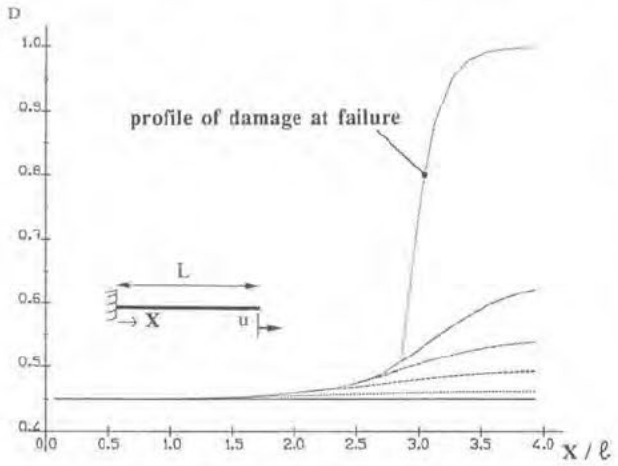

Fig. 5. Evolution of the distribution of damage with the loading in the post-bifurcation regime for a bar.

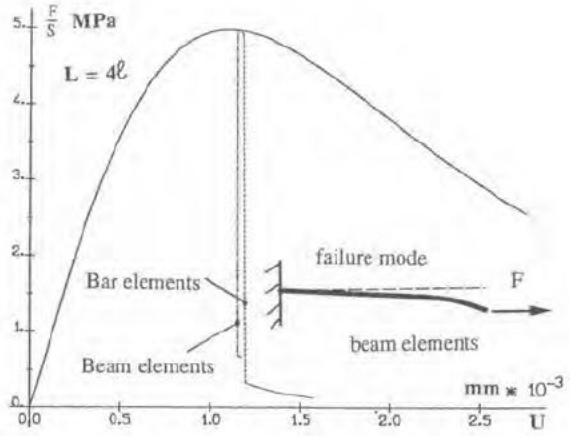

Fig. 6. Comparison between the calculations with bar elements and beam elements on a clamped bar.

the real failure mode is not contained in the finite element model, failure computations cannot yield realistic results. Nevertheless, it is expected that spurious localization due solely to the finite element model as observed in [23] should not be observed. In these situations, one element or group of elements tends to exhibit a sharp localization which is not compatible with the regularization introduced in the nonlocal continuum. The occurrence of such spurious localization modes (eigenmodes) and their importance are presently under investigation.

Finally, Fig. 7 shows a calculation on a beam subjected to four point bending. The beam length is $10l$ and the finite element size is $0.5l$. A standard finite element calculation would show that failure occurs simultaneously in all the elements between the two loads P_1 and P_2. Due to round-off errors, localization can be triggered in one of these elements eventually. In the example presented here, this phenomenon occurs in the midspan element. On the contrary, the bifurcation analysis shows that damage should localize under one of the two points of application of the loads. This is a classical situation in which a symmetric structure loaded by symmetric forces exhibits a non-symmetric failure mode.

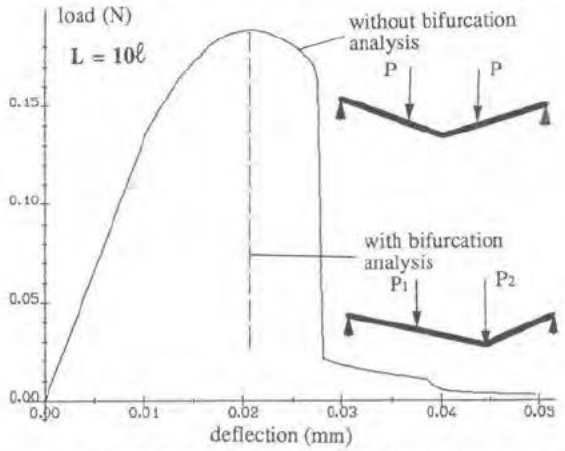

Fig. 7. Response of a four point bending beam.

5. Conclusions

1. Bifurcation and stability analyses of nonlocal strain softening solids have proved that such features as loss of uniqueness and loss of stability of equilibrium solutions may exist despite the implementation of a localization limiter – the nonlocal damage model. These analyses require the computation of the tangent stiffness operator of the structure which appears to be non-symmetric. The computational procedure for the calculation of this matrix within the finite element method has been exposed.

2. The eigenmode analysis and perturbation method proposed by De Borst to study the bifurcation and post-bifurcation response of classical (local) strain-softening structure has been extended to the case in which the tangent stiffness operator is non-symmetric. Uniqueness and stability yield two separate conditions: uniqueness is lost if the tangent operator is singular, stability can be lost only when the symmetric part of the stiffness matrix becomes singular. These conditions are rarely satisfied at the same time.

3. In numerical computations, the condition for loss of stability is monitored only. This is also the most restrictive condition. A perturbation method which uses the eigenvector of the symmetric part of the tangent stiffness matrix is used afterwards to obtain the stable equilibrium path of the structure.

4. The results show that the number of possible solutions at a bifurcation point is very restricted due to the constraint introduced by the spatial averaging in the nonlocal model. The response of the structure is still mesh independent, including the location of the bifurcation and loss of stability points. Nevertheless, the finite element model can still provide incorrect results: (i) when the kinematic of the failure mode is not contained in the finite element model, it cannot be accurately reproduced; (ii) when finite element calculations take advantage of the geometrical and loading symmetries and deal only with the discretization of a portion of structure, results should be interpreted with caution as far as the failure modes are concerned. These modes may not belong to the stable response of the structure and the ductility and energy dissipated at failure can be seriously overestimated.

Acknowledgment

Partial support from the EURO-GRECO on Geomaterials, Project: Numerical Modelling of Strain Softening in Concrete, under the auspices of the Commission of the European Community (Program SCIENCE) is gratefully acknowledged. Thanks are also due to Mr. L. Bodé for helping us with the computer graphics and to Dr. R. Billardon for stimulating discussions.

References

[1] J. Mazars and Z.P. Bazant, eds, Cracking and Damage (Elsevier, Barking, 1989).
[2] A. Needleman, Material rate dependence and mesh sensitivity in localization problems, Comput. Methods Appl. Mech. Engrg. 67 (1) (1988) 69–85.
[3] T. Belytschko and J. Fish, Spectral superposition on finite elements for shear banding problems, in: R. Gruber

et al., eds., Proc. 5th Internat. Symposium on Numerical Methods in Engineering Vol. 1 (Springer, Berlin, 1989) 19–29.
[4] R. De Borst, Simulation of localization using Cosserat theory, in: N. Bicanic and H. Mang, eds., Proc. 2nd Internat. Conf. on Computer Aided Analysis and Design of Concrete Structures (Pineridge, Swansea, 1990) 931–944.
[5] Z.P. Bazant and J. Ozbolt, Nonlocal microplane model for fracture, damage and size effect in structures, Report No. 89–10/498n, ACBM, Northwestern University, Evanston, IL, USA, 1989.
[6] H.L. Schreyer and Z. Chen, One dimensional softening with localization, ASME J. Appl. Mech. 53 (1986) 791–797.
[7] G. Pijaudier-Cabot, Z.P. Bazant and M. Tabbara, Comparison of various models for strain softening, Engrg. Comput. 5 (1988) 141–150.
[8] Z.P. Bazant and G. Pijaudier-Cabot, Nonlocal continuum damage, localization instability and convergence, ASME J. Appl. Mech. 55 (1988) 287–293.
[9] C. Saouridis, Identification et numérisation objectives des comportments adoucissants: Une approche multiéchelle de l'endommagement du béton, Thèse de Doctorat, Université Paris VI, 1989.
[10] R. De Borst, Computation of post-bifurcation and post failure behavior of strain softening solids, Comput. & Structures 25 (2) (1987) 211–224.
[11] R. De Borst, Bifurcation in finite element models with a non-associated flow law, Internat. J. Numer. Analyt. Methods Geomech. 12 (1988) 99–116.
[12] G. Pijaudier-Cabot and Z.P. Bazant, Nonlocal damage theory, ASCE J. Engrg. Mech. 113 (10) (1987) 1512–1533.
[13] J. Mazars and G. Pijaudier-Cabot, Continuum damage theory: Application to concrete, ASCE J. Engrg. Mech. 115 (2) (1989) 345–365.
[14] G. Pijaudier-Cabot and Y. Berthaud, Effet des interactions dans l'endommagement d'un milieu fragile, C.R. Acad. Sci. Paris, t. 310, Serie II (1990) 1577–1582.
[15] G. Pijaudier–Cabot and Z.P. Bazant, Cracks interacting with particles or fibers in composite materials, Int. Report No. 105, Laboratoire de Mécanique et Technologie/NSF Center for Advanced Cement Based Materials, June 1990; also ASCE J. Engrg. Mech. 117 (7) (1991) 1611–1630.
[16] Z.P. Bazant and G. Pijaudier-Cabot, Measurement of the characteristic length of nonlocal continuum, ASCE J. Engrg. Mech. 115 (4) (1989) 757–767.
[17] Z.P. Bazant, J.Y. Pan and G. Pijaudier-Cabot, Strain softening in reinforced concrete beams and frames, ASCE J. Struct. Engrg. 113 (12) (1987) 2333–2347.
[18] J. Rudnicki and J.R. Rice, A note on some features of the theory of localization of deformation, Internat. J. Solids and Structures 16 (1980) 597–605.
[19] A. Benallal, R. Billardon and G. Geymonat, Some mathematical aspects of the damage softening rate problem, in: J. Mazars and Z.P. Bazant, eds., Cracking and Damage (Elsevier, Amsterdam, 1989) 247–258.
[20] K. Willam and G. Etse, Assessment of the extended leon model for plain concrete, in: N. Bicanic and H. Mang, eds., Proc. 2nd Internat. Conf. on Computer Aided Analysis and Design of Concrete Structures (Pineridge, Swansea, 1990) 851–870.
[21] R. Hill, Some basic principles in the mechanics of solids without a natural time, J. Mech. Phys. Solids 7 (1959) 209–225.
[22] H.W. Reinhardt, H.A.W. Cornelissen and D.A. Hordijk, Tensile tests and failure analysis of concrete, ASCE J. Structural Engrg. 112 (11) (1986) 2462–2474.
[23] R. De Borst, Analysis of spurious kinematic modes in finite element analysis of strain softening solids, in: J. Mazars and Z.P. Bazant, eds. Cracking and Damage (Elsevier, Amsterdam, 1989) 335–348.